

# Vector and Axial-Vector Mesons in Nuclear Matter

Ralf-Arno Tripolt<sup>1,2</sup>

in collaboration with

Tetyana Galatyuk<sup>2,3,4</sup>, Lorenz von Smekal<sup>1,2</sup>, Jochen Wambach<sup>3</sup>, Maximilian Wiest<sup>3,4</sup>

<sup>1</sup>JLU Giessen, <sup>2</sup>HFHF, <sup>3</sup>TU Darmstadt, <sup>4</sup>GSI

Workshop “From first-principles QCD to experiments”

ECT\*, Trento, May 22-26, 2023



# Trento



# ECT\* Workshop



## I) Introduction and motivation

- ▶ heavy-ion collisions, QCD phase diagram, dileptons

## II) Theoretical setup

- ▶ Functional Renormalization Group
- ▶ parity-doublet model
- ▶ spectral functions with the aFRG method

## III) Results on spectral functions and dileptons

- ▶ in-medium  $\rho$  and  $a_1$  spectral functions
- ▶ thermal dilepton rates and spectra

## IV) Summary and outlook

## Introduction and motivation

# QCD phase diagram

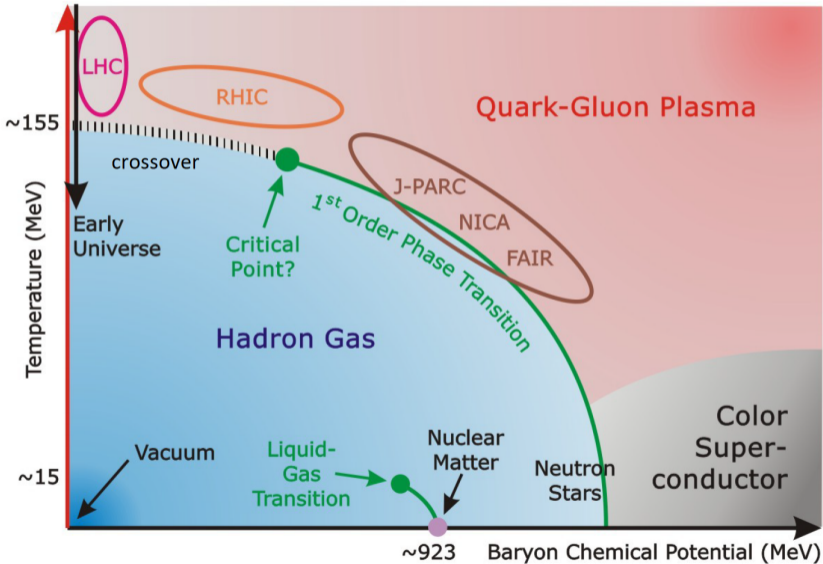


[Figure adapted from the CRC-TR 211 funding proposal]

# Dileptons in heavy-ion collisions

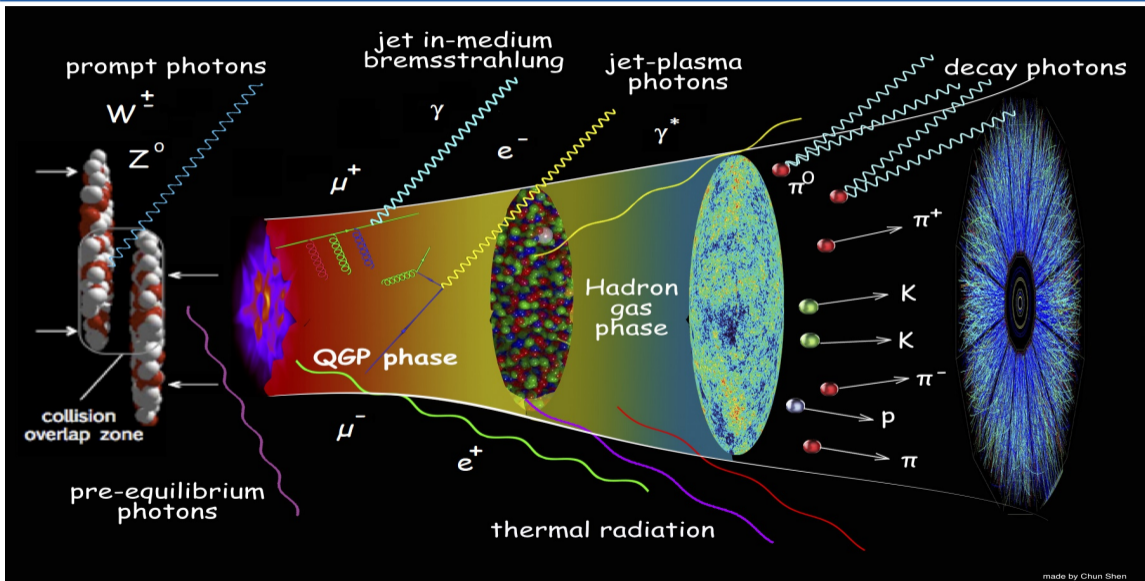
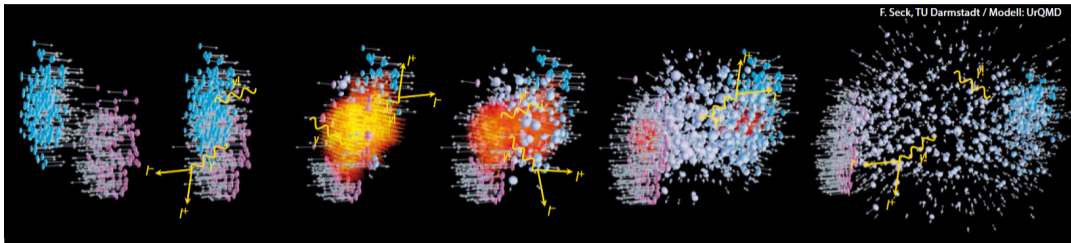


[Figure by Chun Shen]

# Why dileptons?



- ▶ Electromagnetic (EM) probes, i.e. photons and dileptons, don't interact 'strongly' with medium
  - ▶ they have a long mean free path and can carry information from production site to detectors
  - ▶ they are produced at all stages of the collision
- **dileptons are uniquely well-suited to study hot and dense matter in heavy-ion collisions!**

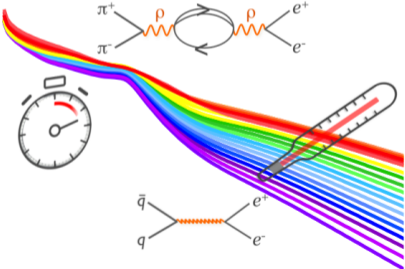




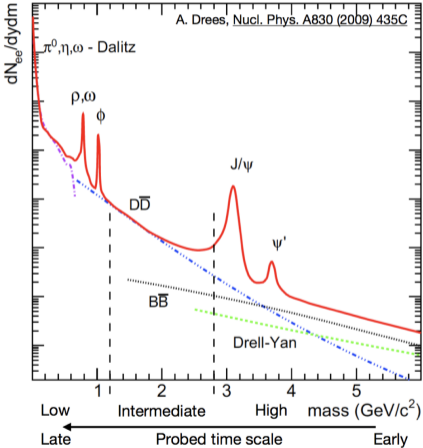
# What can we learn from dileptons?

## Dileptons contain information on:

- ▶ temperature, fireball lifetime, in-medium spectral functions, chiral symmetry, changes in degrees of freedom, transport coefficients (electrical conductivity), ...



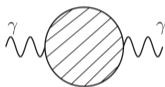
[T. Galatyuk, H. v. Hees, R. Rapp, J. Wambach, Physik Journal 17, Nr. 10 (2018)]



# Dilepton production rates

**Thermal field theory:** Electromagnetic correlation function

$$\Pi_{\text{EM}}^{\mu\nu}(M, p; \mu_B, T) = -i \int d^4x e^{ip \cdot x} \Theta(x_0) \langle\langle [j_{\text{EM}}^\mu(x), j_{\text{EM}}^\nu(0)] \rangle\rangle$$



determines both **photon and dilepton rates**:

▶ photons: 
$$p_0 \frac{dN_\gamma}{d^4x d^3p} = -\frac{\alpha_{\text{EM}}}{\pi^2} f^B(p_0; T) \frac{1}{2} g_{\mu\nu} \text{Im} \Pi_{\text{EM}}^{\mu\nu}(M = 0, p; \mu_B, T),$$

▶ dileptons: 
$$\frac{dN_{ll}}{d^4x d^4p} = -\frac{\alpha_{\text{EM}}^2}{\pi^3 M^2} L(M) f^B(p_0; T) \frac{1}{3} g_{\mu\nu} \text{Im} \Pi_{\text{EM}}^{\mu\nu}(M, p; \mu_B, T),$$

# EM spectral function in the vacuum

In the vacuum,  $\text{Im} \Pi_{\text{em}}^{\text{vac}}$  is accurately known from  $e^+e^-$  annihilation:

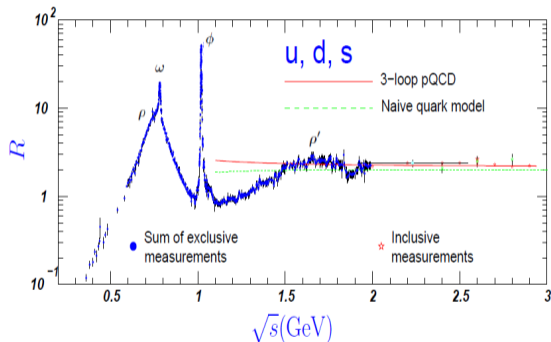
$$R = \frac{\sigma(e^+e^- \rightarrow \text{hadrons})}{\sigma(e^+e^- \rightarrow \mu^+\mu^-)} \propto \frac{\text{Im} \Pi_{\text{em}}^{\text{vac}}}{M^2}$$

In the low-mass regime (LMR:  $M \leq 1$  GeV) the EM spectral function is saturated by the **spectral functions of the light vector mesons (VMD)**:

$$\text{Im} \Pi_{\text{EM}}^{\text{vac}}(M) = \sum_{v=\rho,\omega,\phi} \left( \frac{m_v^2}{g_v} \right)^2 \text{Im} D_v^{\text{vac}}(M)$$

For higher energies, quark degrees of freedom:

$$\text{Im} \Pi_{\text{EM}}^{\text{vac}}(M) = -\frac{M^2}{12\pi} \left[ 1 + \frac{\alpha_s(M)}{\pi} + \dots \right] N_c \sum_{q=u,d,s} (e_q)^2$$



[Particle Data Group]

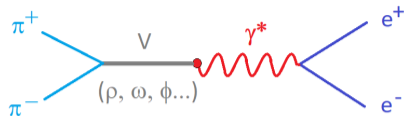
[J.J. Sakurai, Ann.Phys. 11 (1960) & Currents and Mesons, Chicago Lectures]

[R. Rapp, J. Wambach, Adv.Nucl.Phys. 25, 1 (2000)]

[R. Rapp, Acta Phys.Polon. B42, 2823-2852 (2011)]

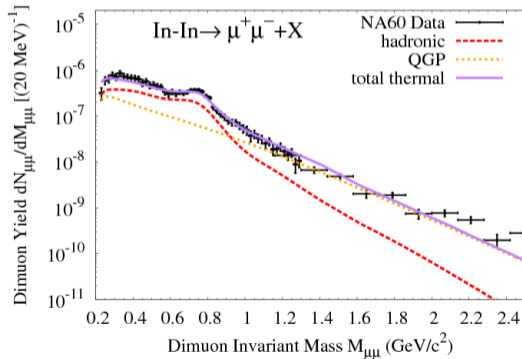
# Connection between dileptons and vector mesons

Vector mesons have the same quantum numbers as photons and can decay directly into dileptons:



Excess dimuon invariant-mass spectrum as measured in In-In collisions at  $\sqrt{s_{NN}} = 17.3$  GeV by the NA60 collaboration at the SPS is well described by using **vector meson dominance**:

$$\text{Im}\Pi_{\text{EM}}^{\mu\nu}(M) \sim \text{Im}D_{\rho}^{\mu\nu} + \frac{1}{9}\text{Im}D_{\omega}^{\mu\nu} + \frac{2}{9}\text{Im}D_{\phi}^{\mu\nu}$$



# Connection of (axial-)vector mesons and chiral symmetry

## Chiral symmetry:

- ▶ QCD Lagrangian has chiral symmetry  $SU(N_f)_L \times SU(N_f)_R$  in the limit of vanishing quark masses
- ▶ chiral symmetry is broken spontaneously by dynamical formation of a quark condensate  $\langle \bar{q}q \rangle \sim \Delta_{l,s}$

## QCD and chiral sum rules:

$$\int_0^\infty \frac{ds}{\pi} (\Pi_V(s) - \Pi_A(s)) = m_\pi^2 f_\pi^2 = -2m_q \langle \bar{q}q \rangle$$

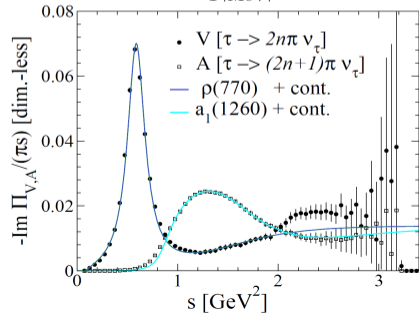
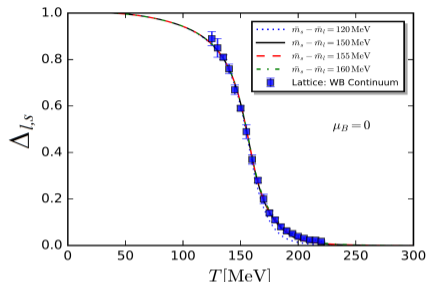
- ▶ sum rules connect spectral functions and condensates
- ▶ chiral restoration manifests itself through mixing of vector and axial-vector correlators!

[W.-j. Fu, J.M. Pawłowski, F. Rennecke, Phys. Rev. D 101, 054032 (2020)]

[S. Borsanyi et al. (Wuppertal-Budapest), JHEP 09, 073 (2010)]

[R. Barate, et al., (ALEPH), EPJC 4 (1998) 409-431]

[R. Rapp, J. Wambach, H. v. Hees, Landolt-Bornstein 23, 134]



# Chiral Mixing

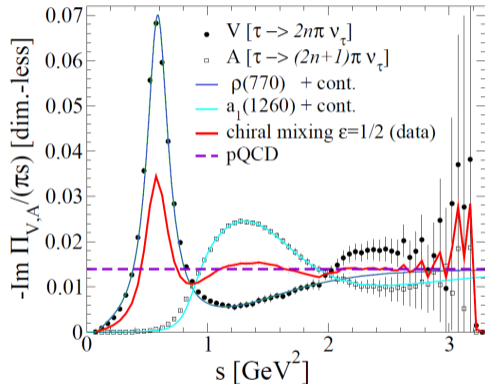
At low temperatures and densities, i.e. for a dilute pion gas, one can apply chiral reduction and current algebra to find the following 'mixing theorem' for the vector and axial-vector correlation functions:

$$\Pi_V(q) = (1 - \varepsilon) \Pi_V^0(q) + \varepsilon \Pi_A^0(q)$$

with mixing parameter  $\varepsilon = T^2/6f_\pi^2$ .

Chiral mixing has direct consequences on the thermal dilepton rate:

$$\frac{dN_{ll}}{d^4x d^4q} = \frac{4\alpha_{EM}^2 f^B}{(2\pi)^2} \left\{ \rho_{EM} - \left( \varepsilon - \frac{\varepsilon^2}{2} \right) (\rho_V - \rho_A) \right\}$$



[R. Rapp, Acta Phys. Polon. B 42 (2011) 2823-2852]

[M. Dey et al., Phys. Lett. B 252 (1990), 620-624]

[Z. Huang, Phys. Lett. B 361 (1995) 131-136]

### Theoretical setup

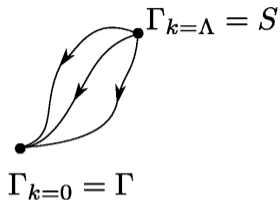


# Method of choice: FRG

## Functional Renormalization Group (FRG):

$$\partial_k \Gamma_k = \frac{1}{2} \text{STr} \left( \partial_k R_k \left[ \Gamma_k^{(2)} + R_k \right]^{-1} \right)$$

[C. Wetterich, Phys.Lett. B301, 90 (1993)]



[wikipedia.org]

- ▶ non-perturbative continuum framework
- ▶ implements Wilson's coarse-graining idea: fluctuations integrated out
- ▶  $\Gamma_k$  interpolates between bare action  $S$  in the UV and effective action  $\Gamma$  in the IR
- ▶ capable of describing phase transitions at finite temperature and density
- ▶ **analytically-continued FRG (aFRG) method gives access to spectral functions!**

# Effective theory for nuclear matter

---

We use the **parity-doublet model** with  $N_1 = N(938) = (n, p)$ ,  $N_2 = N^*(1535)$ :

$$\Gamma_k = \int d^4x \left\{ \bar{N}_1 (\not{\partial} - \mu_B \gamma_0 + h_1(\sigma + i\vec{\tau} \cdot \vec{\pi} \gamma^5)) N_1 + \bar{N}_2 (\not{\partial} - \mu_B \gamma_0 + h_2(\sigma - i\vec{\tau} \cdot \vec{\pi} \gamma^5)) N_2 \right. \\ \left. + m_{0,N} (\bar{N}_1 \gamma^5 N_2 - \bar{N}_2 \gamma^5 N_1) + U_k(\phi^2) - c\sigma \right\}$$

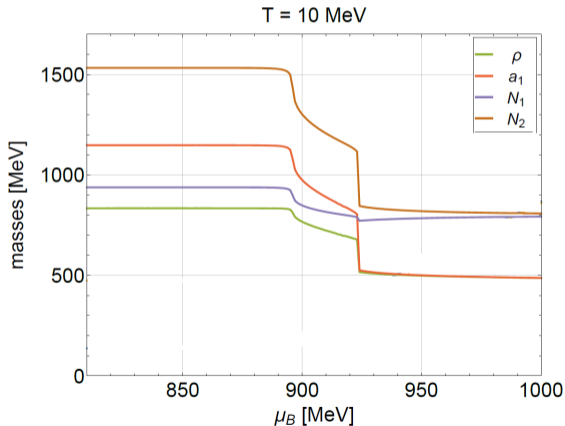
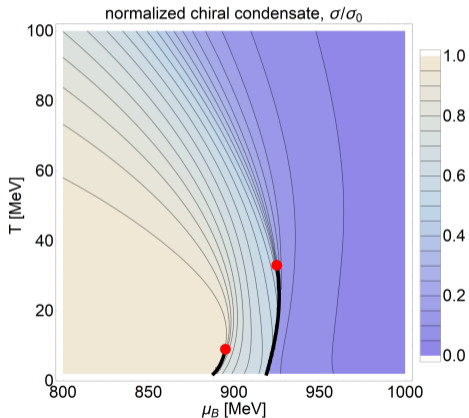
- ▶ provides a phenomenologically successful description of nuclear matter
- ▶ describes **nuclear liquid-gas transition together with a chiral phase transition**
- ▶ accounts for a **finite nucleon mass**  $m_{0,N}$  in a **chirally-invariant** fashion
- ▶ provides a natural description for the **parity-doubling structure** of the low-lying baryons

[C. E. Detar, T. Kunihiro, Phys. Rev. D 39, 2805 (1989)]

[R.-A. T., C. Jung, L. v. Smekal, J. Wambach, Phys. Rev. D 104, 054005 (2021)]

# Parity-doublet model (I)

- ▶ describes nuclear liquid-gas transition together with a chiral phase transition:



# Parity-doublet model (II)

Accounts for a **finite nucleon mass in a chirally-invariant fashion**:

- ▶ the **proton mass** can be obtained from the trace of the energy-momentum tensor of QCD

$$T \equiv T_{\mu}^{\mu} = \frac{\beta(g)}{2g} G^{\mu\nu a} G_{\mu\nu}^a + \sum_{l=u,d,s} m_l (1 + \gamma_{m_l}) \bar{q}_l q_l$$
$$\rightarrow \langle \mathbf{p}_1 | T | \mathbf{p}_2 \rangle \sim G(q^2), \quad G(0) = M$$

with the scalar gravitational form factor  $G$

- ▶ only  $\sim 8\%$  from chiral symmetry breaking ('sigma-term'), **rest from gluon term!**
- ▶ **mass radius of the proton** can be obtained as derivative w.r.t. momentum transfer  $t = q^2$ :

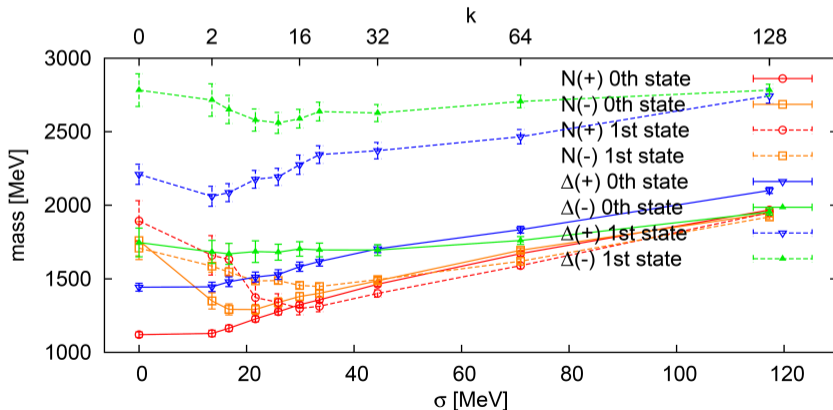
$$\langle R_m^2 \rangle = \frac{6}{M} \left. \frac{dG}{dt} \right|_{t=0}$$

→ GlueX data leads to  $R_m \approx 0.55$  fm, as opposed to  $R_c \approx 0.84$  fm!

# Parity-doublet model (III)

Provides a natural description for the parity-doubling structure of the low-lying baryons:

- ▶ lattice simulations show **degeneration of parity partners** as chiral symmetry is (artificially) restored by removing the  $k$  lowest Dirac modes:



# Introducing vector and axial-vector mesons

## Parity-doublet model with vector mesons:

$$\begin{aligned}\Gamma_k = \int d^4x \left\{ \bar{N}_1 \left( \not{\partial} - \mu_B \gamma_0 + h_{s,1}(\sigma + i\vec{\tau} \cdot \vec{\pi} \gamma^5) + h_{v,1}(\gamma_\mu \vec{\tau} \cdot \vec{\rho}_\mu + \gamma_\mu \gamma^5 \vec{\tau} \cdot \vec{a}_{1,\mu}) \right) N_1 \right. \\ + \bar{N}_2 \left( \not{\partial} - \mu_B \gamma_0 + h_{s,2}(\sigma - i\vec{\tau} \cdot \vec{\pi} \gamma^5) + h_{v,2}(\gamma_\mu \vec{\tau} \cdot \vec{\rho}_\mu - \gamma_\mu \gamma^5 \vec{\tau} \cdot \vec{a}_{1,\mu}) \right) N_2 \\ + m_{0,N} \left( \bar{N}_1 \gamma^5 N_2 - \bar{N}_2 \gamma^5 N_1 \right) + U_k(\phi^2) - c\sigma + \frac{1}{2} (D_\mu \phi)^\dagger D_\mu \phi \\ \left. - \frac{1}{4} \text{tr} \partial_\mu \rho_{\mu\nu} \partial_\sigma \rho_{\sigma\nu} + \frac{m_v^2}{8} \text{tr} \rho_{\mu\nu} \rho_{\mu\nu} \right\}.\end{aligned}$$

- ▶  $\rho$  and  $a_1$  in terms of **anti-symmetric rank-2 tensor fields** which transform according to the (1,0) and (0,1) representations of the Euclidean O(4) group (with generators  $T_R$  and  $T_L$ ):

$$\rho_{\mu\nu} = \rho_{\mu\nu}^+ + \rho_{\mu\nu}^- = \vec{\rho}_{\mu\nu}^+ \vec{T}_R + \vec{\rho}_{\mu\nu}^- \vec{T}_L$$

- ▶ the iso-triplet **vector and axial-vector fields** are obtained as

$$\vec{\rho}_\mu = \frac{1}{2m_v} \text{tr}(\partial_\sigma \rho_{\sigma\mu} \vec{T}_V), \quad \vec{a}_{1\mu} = \frac{1}{2m_v} \text{tr}(\partial_\sigma \rho_{\sigma\mu} \vec{T}_A)$$

# Flow equations for $\rho$ and $a_1$ 2-point functions

$$\begin{aligned}
 \partial_k \Gamma_{\rho, k}^{(2)} = & \text{Diagram 1} + \text{Diagram 2} + \text{Diagram 3} - 2 \text{Diagram 4} - \frac{1}{2} \text{Diagram 5} \\
 \partial_k \Gamma_{a_1, k}^{(2)} = & \text{Diagram 6} + \text{Diagram 7} + \text{Diagram 8} + \text{Diagram 9} - 2 \text{Diagram 10} \\
 & + \text{Diagram 11} + \text{Diagram 12} - \frac{1}{2} \text{Diagram 13} - \frac{1}{2} \text{Diagram 14}
 \end{aligned}$$

The diagrams represent various loop topologies for the flow equations. Diagram 1: Loop with vertices  $\rho$  and  $\pi$ . Diagram 2: Loop with vertices  $\rho$  and  $a_1$ . Diagram 3: Loop with vertices  $\rho$  and  $a_1$  (dashed lines). Diagram 4: Loop with vertices  $\rho$  and  $N$ . Diagram 5: Loop with vertices  $\rho$  and  $\pi$  (dashed lines). Diagram 6: Loop with vertices  $a_1$  and  $\sigma$ . Diagram 7: Loop with vertices  $a_1$  and  $\pi$ . Diagram 8: Loop with vertices  $a_1$  and  $\rho$  (dashed lines). Diagram 9: Loop with vertices  $a_1$  and  $\rho$  (dashed lines). Diagram 10: Loop with vertices  $a_1$  and  $N$ . Diagram 11: Loop with vertices  $a_1$  and  $\sigma$  (dashed lines). Diagram 12: Loop with vertices  $a_1$  and  $a_1$  (dashed lines). Diagram 13: Loop with vertices  $a_1$  and  $\pi$  (dashed lines). Diagram 14: Loop with vertices  $a_1$  and  $\sigma$  (dashed lines).

- ▶ vertices extracted from ansatz for the effective average action  $\Gamma_k$
- ▶ **aFRG method** allows for **analytic continuation** of flow equations to real energies  $\omega$ !

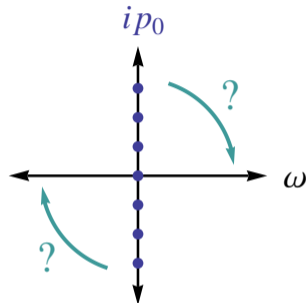
# Two-step analytic continuation procedure

1) Use periodicity w.r.t. imaginary energy  $ip_0 = i2n\pi T$ :

$$n_{B,F}(E + ip_0) \rightarrow n_{B,F}(E)$$

2) Substitute  $p_0$  by continuous real frequency  $\omega$ :

$$\Gamma^{(2),R}(\omega, \vec{p}) = -\lim_{\epsilon \rightarrow 0} \Gamma^{(2),E}(ip_0 \rightarrow -\omega - i\epsilon, \vec{p})$$



Spectral function is then given by

$$\rho(\omega, \vec{p}) = -\frac{1}{\pi} \text{Im} \frac{1}{\Gamma^{(2),R}(\omega, \vec{p})}$$

[K. Kamikado, N. Strodthoff, L. von Smekal, J. Wambach, Eur.Phys.J. C74 (2014) 2806]

[R.-A. T., N. Strodthoff, L. v. Smekal, and J. Wambach, Phys. Rev. D **89**, 034010 (2014)]

[J. M. Pawłowski, N. Strodthoff, Phys. Rev. D **92**, 094009 (2015)]

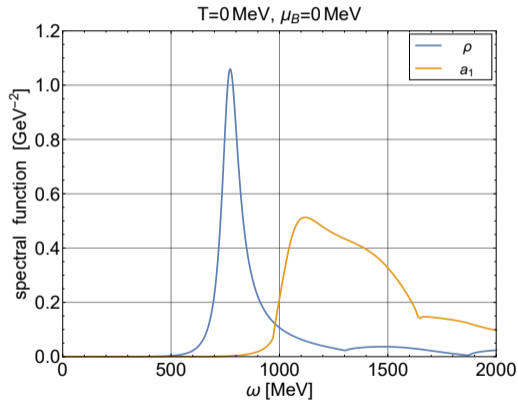
[N. Landsman and C. v. Weert, Physics Reports 145, 3&4 (1987) 141]



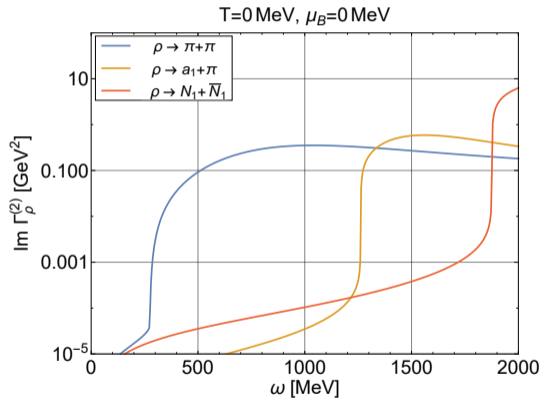
### Results on spectral functions and dileptons

# $\rho$ and $a_1$ spectral functions in the vacuum (aFRG)

spectral functions:



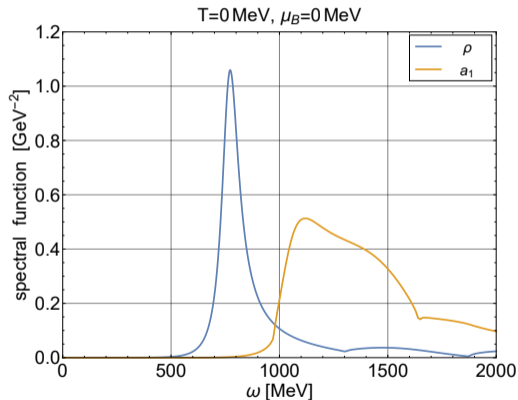
imaginary part of  $\rho$  2-point function:



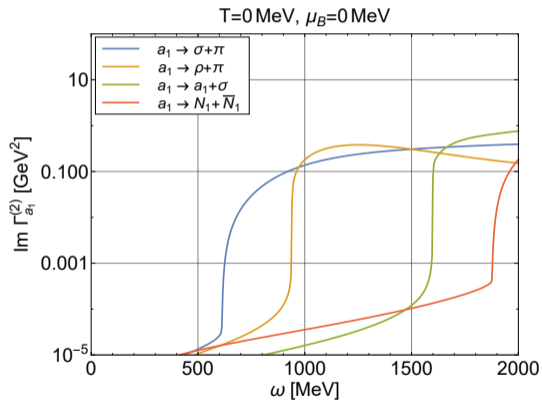
[R.-A. T., C. Jung, L. von Smekal, J. Wambach, Phys. Rev. D 104, 054005 (2021)]

# $\rho$ and $a_1$ spectral functions in the vacuum (aFRG)

spectral functions:



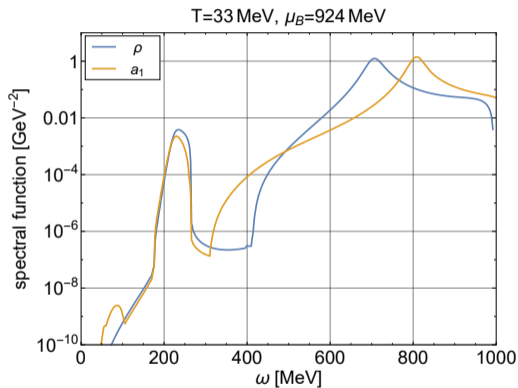
imaginary part of  $a_1$  2-point function:



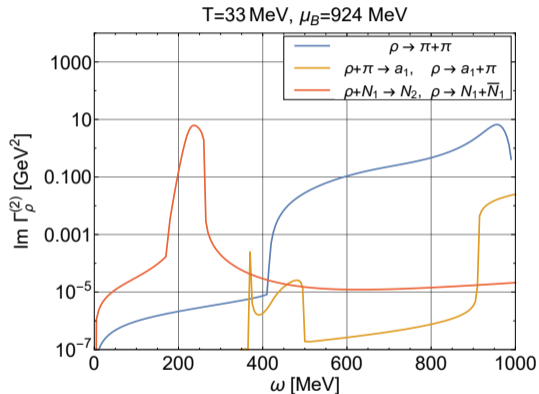
[R.-A. T., C. Jung, L. von Smekal, J. Wambach, Phys. Rev. D 104, 054005 (2021)]

# $\rho$ and $a_1$ spectral functions near chiral CEP (aFRG)

spectral functions:



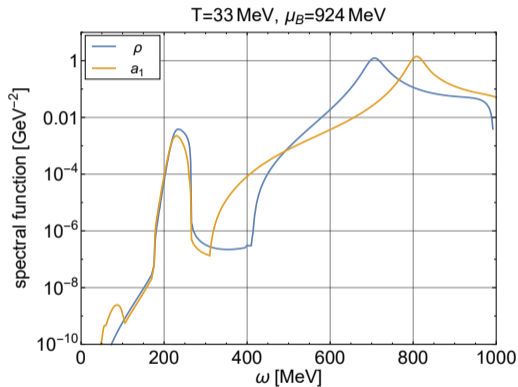
imaginary part of  $\rho$  2-point function:



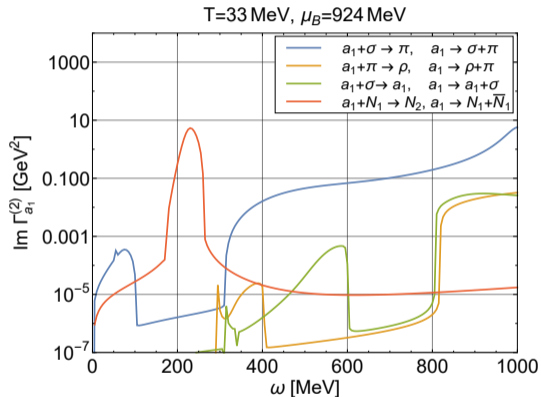
► a pronounced peak at lower energies due to the process  $\rho + N_1 \rightarrow N_2$  is observed!

# $\rho$ and $a_1$ spectral functions near chiral CEP (aFRG)

spectral functions:

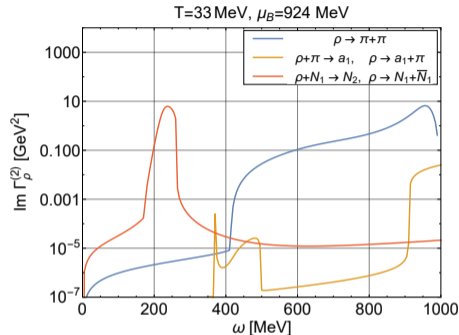
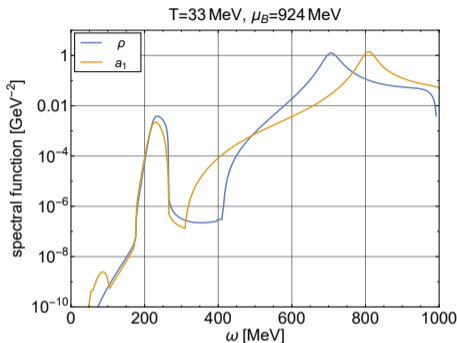


imaginary part of  $a_1$  2-point function:



► a pronounced peak at lower energies due to the process  $a_1 + N_1 \rightarrow N_2$  is observed!

# $\rho$ and $a_1$ spectral functions near chiral CEP



- peak due to process  $\rho + N \rightarrow N^*(1535)$ , depends on size of  $\rho$ - $N$ - $N^*(1535)$  coupling:

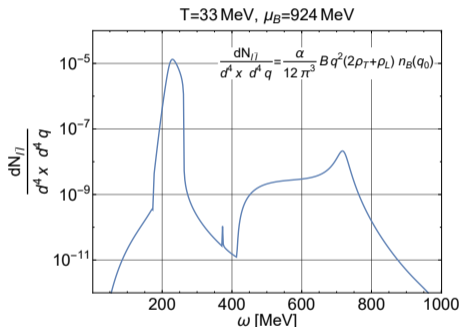
## $N(1535)$ BRANCHING RATIOS

$\Gamma(N\rho, S=1/2)/\Gamma_{\text{total}}$				$\Gamma_7/\Gamma$
VALUE (%)	DOCUMENT ID	TECN	COMMENT	
$2.7 \pm 0.6$	ADAMCZEW... 20	DPWA	Multichannel	
$14 \pm 2$	<sup>11</sup> HUNT 19	DPWA	Multichannel	

# Preliminary results on dilepton rate and spectrum

The resonance-production peak in the  $\rho$  spectral function due to the process  $\rho + N \rightarrow N^*(1535)$  directly translates into an **enhancement of the thermal dilepton rate**:

dilepton rate from Weldon formula:

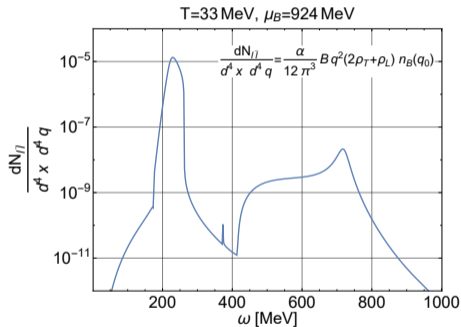


- ▶ unique **prediction of the parity-doublet model!**
- ▶ detection would yield strong evidence in support of the parity-doubling scenario as providing the mechanism for chiral symmetry restoration in dense nuclear matter!

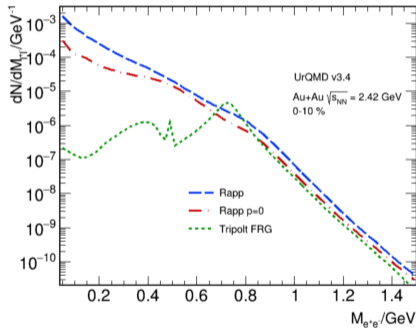
# Preliminary results on dilepton rate and spectrum

The resonance-production peak in the  $\rho$  spectral function due to the process  $\rho + N \rightarrow N^*(1535)$  directly translates into an **enhancement of the thermal dilepton rate**:

dilepton rate from Weldon formula:



dilepton spectrum from UrQMD and coarse-grainig (Max Wiest):



- ▶ unique **prediction of the parity-doublet model!**
- ▶ detection would yield strong evidence in support of the parity-doubling scenario as providing the mechanism for chiral symmetry restoration in dense nuclear matter!

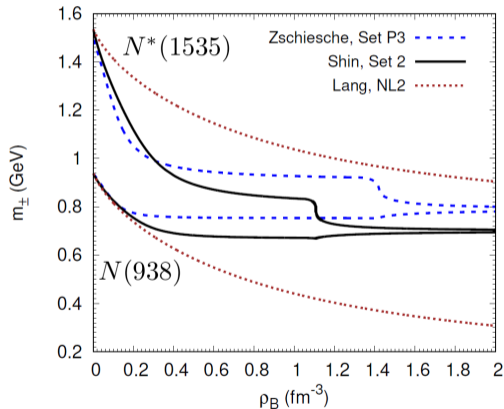


# Transport simulation with parity doubling

Parity-doublet model (PDM) mean fields for the nucleon,  $N(938)$ , and its parity partner,  $N^*(1535)$ , were included in the GiBUU microscopic transport model:

- ▶ red-dotted line: Walecka mean fields (NL2)
- ▶ black and blue-dashed lines: PDM mean fields (Set 2 and P3)
- ▶ mass of the  $N^*(1535)$  resonance decreases quickly with increasing baryon density  $\rho_B$  for the PDM fields

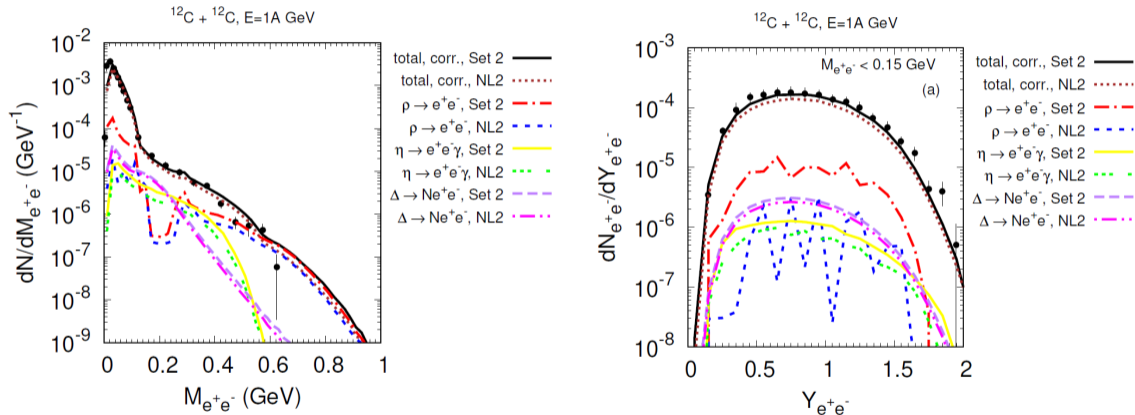
→ **leads to enhancement of  $N^*(1535)$  production in the intermediate stages of central heavy-ion collisions at 1 AGeV!**



[A. B. Larionov, L. von Smekal, Phys. Rev. C 105, 034914 (2022)]

# Transport simulation with parity doubling

Invariant-mass and rapidity distributions of dileptons in C+C collisions at 1 AGeV with GiBUU:



→ **PDM mean fields lead to enhanced  $\rho \rightarrow e^+e^-$  and  $\eta \rightarrow e^+e^-\gamma$  signals!**

# Summary and Outlook

---

We computed  $\rho$  and  $a_1$  spectral functions in nuclear matter:

- ▶ based on the parity-doublet model and the aFRG method
- ▶ effects of chiral symmetry restoration lead to peak in spectral functions at low energies
- ▶ might be observed experimentally in terms of increased dilepton yield!

## Outlook:

- ▶ include repulsive effect ( $\sim \omega$ ) for realistic description of nuclear matter
- ▶ include isospin-chemical potential to describe neutron-rich matter
- ▶ compute equation of state and thermal neutrino rates